The interplay between iron limitation, light, and carbon in the proteorhodopsin containing Photobacterium angustum S14

Coco Koedooder, Rémy van Geersdaële, Audrey Gueneugues, François-Yves Bouget, Ingrid Obernosterer, Stephane Blain

The interplay between iron limitation, light, and carbon in the proteorhodopsin containing *Photobacterium angustum* S14

Coco Koedooder[1,2*], Rémy Van Geersdaële[1], Audrey Guéneuguès[1], François-Yves Bouget[1], Ingrid Obernosterer[1], Stéphane Blain[1]

[1]*Sorbonne Université, UPMC Univ Paris 06, CNRS, Laboratoire d'Océanographie Microbienne (LOMIC), Observatoire Océanologique, Banyuls/mer, France*
[2] *The Fredy and Nadine Herrmann Institute of Earth Sciences, Hebrew University of Jerusalem, Jerusalem, Israel*

Keywords: proteorhodopsin, Fe-limitation, *Photobacterium angustum* S14, photoheterotrophy

Abstract

Fe-limitation is known to affect heterotrophic bacteria within the respiratory electron transport chain, therefore strongly impacting the overall intracellular energy production. We investigated whether the gene expression pattern of the light-sensitive proton pump, proteorhodopsin (PR), is influenced by varying light, carbon and Fe-concentrations in the marine bacterium Photobacterium angustum S14 and whether PR can alleviate the physiological processes associated with Fe-starvation. Our results show that the gene expression of PR increases as cells enter the stationary phase, irrespective of Fe-replete or Fe-limiting conditions. This upregulation is coupled to a reduction in cell size, indicating that PR gene regulation is associated with a specific starvation-stress response. We provide experimental evidence that PR gene expression does not result in an increased growth rate, cell abundance, enhanced survival or ATP concentration within the cell in either Fe-replete or Fe-limiting conditions. However, independent of PR gene expression, the presence of light did influence bacterial growth rates and maximum cell abundances under varying Fe-regimes. Our observations support previous results indicating that PR phototrophy seems to play an important role within the stationary phase for several members of the Vibrionaceae family, but that the exact role of PR in Fe-limitation, remains to be further explored.

[*] ***corresponding author details:***
Coco Koedooder
cocokoedooder@gmail.com
The Fredy and Nadine Herrmann Institute of Earth Sciences, Hebrew University of Jerusalem, Jerusalem, Israel

1. Introduction

Iron (Fe) is an essential trace element in organisms due to its ability to harbour two major oxidation states, and the various enzymes that require Fe for their functioning are responsible for major cellular processes including photosynthesis, respiration, DNA synthesis and nitrogen fixation (Merchant and Helmann 2012; Ilbert and Bonnefoy 2013). Fe in the ocean is present in various chemical forms and redox states, and experiences a multitude of transformations mediated by chemical, physical and biological processes that will ultimately determine both its solubility and bioavailability towards the microorganisms present within the water column (Lis *et al.* 2015; Blain and Tagliabue 2016; Tagliabue *et al.* 2017). Heterotrophic bacteria, like all other organisms, are affected by Fe-limitation which will subsequently impact the biogeochemical cycling of carbon through their role as principal remineralizers of dissolved organic carbon (Azam. F. *et al.* 1983). Within heterotrophic bacteria, the majority of Fe-containing enzymes (~90%) are located within the complexes of the respiratory electron transport chain in the form of various cytochromes and Fe-sulfur clusters (Holms 1996; Tortell *et al.* 1999; Alberts B, Johnson A, Lewis J 2002; Andrews, Robinson and Rodríguez-Quiñones 2003; Almaas, Oltvai and Barabási 2005). Consequently, Fe-limitation, has been shown to particularly affect heterotrophic bacteria in their ability to produce ATP (Tortell, Maldonado and Price 1996).

Proteorhodopsin (PR), a light-driven transmembrane proton pump, was discovered through the genomic analysis of an uncultivated gammaproteobacterial strain of the ubiquitous SAR86 clade (Béjà et al., 2000; 2001). PR requires the chromophore retinal which, in the presence of light, enables it to undergo a conformational change that allows for the absorption and release of a proton across the cellular membrane. The formation of a proton gradient can be harboured for several different physiological functions (Fuhrman, Schwalbach and Stingl 2008), and

when coupled to ATP synthase, PR activity can result in the transformation of light energy to ATP. The low energetic production costs of PR in comparison to other light harvesting complexes (Raven 2009; Kirchman and Hanson 2013), together with the widespread prevalence of PR in the surface waters of the ocean (Gómez-Consarnau *et al.* 2019), hereby suggested the presence of an important form of photoheterotrophy (Béjà *et al.* 2000, 2001; Pinhassi *et al.* 2016; Song *et al.* 2020).

While the biological function of PR as a light-driven proton pump has been well characterized (Martinez *et al.* 2007; Song *et al.* 2020), the exact physiological function and role of PR has only been tested in a handful of cultivatable strains (Pinhassi et al., 2016). Thus far, experiments conducted on culturable PR-containing bacteria (Supplementary Table 1) have shown that the gene expression pattern of PR can differ between strains, and that PR activity can be attributed to a wide range of physiological functions, including the promotion of growth and its use as a survival mechanism under stressful conditions such as periods of carbon starvation and other forms of nutrient limitation (Fuhrman, Schwalbach and Stingl 2008; Pinhassi *et al.* 2016; Song *et al.* 2020).

Considering that Fe-limitation typically results in a decline in energy levels within the cell (Tortell *et al.* 1999), a possible link may exist between PR-based phototrophy and the ability to enhance energy production within Fe-limited cells (Raven 2009; Marchetti *et al.* 2012, 2015; Sun *et al.* 2017; Cohen *et al.* 2018). The formation of a proton gradient by the PR photosystem does not require Fe, while phototrophic systems containing Type I and Type II reaction centers, such as those found in oxygenic phototrophs, require Fe-containing cytochromes in order to sustain electron flow (Blankenship 2010). The comparison of three closely related Roseobacter strains, indicated that the two strains isolated from Fe-replete regions contained a Type II

reaction centre (bacteriochlorophyll complex), while the strain isolated from an environment characterised by Fe-limitation (Antarctic waters) contained a PR gene (Sun *et al.* 2017). It was hereby suggested that the presence of a PR gene was a potential adaptation for a Roseobacter strain subjected to low Fe-concentrations. PR genes have also been identified in several marine eukaryotes (Marchetti *et al.* 2012) and were shown to be upregulated under Fe-limitation compared to Fe-replete conditions within both the oceanic diatom *Pseudo-nitzschia granii* and the polar sea-ice diatom *Fragilariopsis cylindrus* (Marchetti *et al.* 2015; Cohen *et al.* 2018). Interestingly, this upregulation in both light and dark conditions, did not result in significant differences in the growth rate of *P. granii.* PR was hereby predicted to enable the continued survival of *P. granii* until Fe becomes available again to allow cellular growth (Marchetti *et al.* 2015). Whether a similar prediction can be made for PR-containing bacteria subjected to Fe-limitation has, to our knowledge, not been tested. In this study, we aimed to elucidate the potential role of PR in the presence of Fe-limitation using the model marine bacterium *Photobacterium angustum* S14.

2. Material and Methods

2.1. Strains and Maintenance

A culture of *P. angustum* strain S14 was provided by Prof. S. Kjelleberg (UNSW, Sydney, NSW, Australia) and stored under cryopreservation in the Microbial Observatory of the Laboratoire Arago (MOLA) culture collection (BBCC7451*).* For the bacterial transformation of *P. angustum* S14, cultures were grown and maintained in ZoBell and LB medium or agar as described previously (Bertani 1951; Oppenheimer H. C. and ZoBell 1952; Koedooder *et al.* 2018). *Escherichia coli* strains Π3813 and β3914 were used as plasmid hosts for amplification and transformation by bacterial conjugation respectively (Le Roux *et al.* 2007). Both *E. coli* strains were grown in LB medium and LB agar at 37°C. When necessary 5 µg/mL of

111 chloramphenicol (Cm) for *P. angustum* S14 and 25 µg/mL for *E. coli* strains, thymidine (0.3
112 mM) and diaminopimelate (0.3 mM) were added as supplements to the medium. Induction of
113 the P_{BAD} promoter was achieved through the addition of 0.2% L-arabinose to the growth
114 medium. Conversely, its repression was obtained by the addition of 1% D-glucose.

115

116 For the experimental setup, all strains and genetic constructs were grown in 30 mL Thermo
117 Scientific™ Nalgene™ polycarbonate bottles containing 12 mL Aquil medium supplemented
118 with 6 mM[C] glucose and 5.4µM Fe:EDTA (1:1 ratio, Price *et al.* 1989) and placed in the
119 dark at 20°C, agitated with a stirring rate of 110 rpm. Batches were refreshed at least 2 times
120 prior to the start of the experiment (25 µL of a culture was transferred to a fresh 12 mL batch
121 of Aquil medium every 2 days) in order to remove any traces of Fe and carbon that could be
122 carried over from growth on Zobell or LB medium.

123

124 **2.2. Genetic Constructs**

125 Construction of both a PR gene bioreporter (ptr-luc) and a PR gene knockout (Δpr) was
126 performed in *P. angustum* S14 by allelic exchange using the R6K based pSW7848T suicide
127 vector, as described previously (Le Roux *et al.* 2007; Val *et al.* 2012; Lemire *et al.* 2015;
128 Koedooder *et al.* 2018). Briefly, the pSW7848T plasmid contains the gene insert for allelic
129 exchange which, for the construction of the gene knockout, consists of the upstream and
130 downstream region (500 bp) that encompasses the PR gene of *P. angustum* S14 (EAS63552.1)
131 and, for the construction of the bioreporter, consists of the PR gene fused together with a
132 luciferase gene. The pSW7848T plasmid further contains the RP4 replication origin oriT, the
133 pir-dependent R6K replication origin oriR6K and the resistance gene for the antibiotic Cm, as
134 a selection marker. For the construction of Δpr, the pSW7848T plasmid additionally contains

135 the inducible CcdB toxin which is under control of the P_{BAD} promoter and induced in the
136 presence of arabinose. The assembly of the plasmid construct was performed according to the
137 Gibson Assembly protocol (New England Biolabs, NEB) according to the manufacturer's
138 instructions and inserted into the *E. coli* strain Π3813 for amplification by electroporation.
139 After amplification, the plasmid was extracted and purified prior to its insertion into *E. coli*
140 strain β3914 (Le Roux *et al.* 2007; Lemire *et al.* 2015). The plasmid was subsequently
141 transferred by conjugation from *E. coli* β3914 to the recipient *P. angustum* S14 by a filter
142 mating procedure as described previously (Le Roux, Davis and Waldor 2011) with a
143 donor/recipient ratio of 1:10 ml. The plasmid is integrated into *P. angustum* S14 via
144 homologous recombination and selected for in media containing Cm. The gene knockout Δpr,
145 which contains the P_{BAD} promoter, undergoes a second homologous recombination enabling
146 the removal of the plasmid backbone which is selected for in media containing arabinose. The
147 formation of Δpr and ptr-luc was verified via PCR for the presence or absence of the gene
148 fragment and by sequencing the gene products with the wildtype serving as positive or negative
149 control (Supplementary Fig 1).

150

151 **2.3. Trace metal-controlled conditions**

152 All experiments were conducted under trace metal clean conditions in a clean room (class
153 10000) and under a laminar flow hood (ADS class 100; Morel *et al.* 2008). Briefly, all plastic
154 materials were made trace metal free by soaking them for 24 h in 10% HCl. This was followed
155 by rinsing and soaking the materials for another 24 h in an ultra-pure water (UPW) bath that
156 was produced with an 18.2 MΩ cm, Elga system equipped with a 0.2 µm final filter (Thermo
157 Fisher Scientific). Nalgene^{TM} polycarbonate flasks dedicated to the culture experiments were
158 additionally microwaved 3 times at 750 W until boiling with UPW. All plastic materials were
159 placed under the laminar flow hood to dry and sterilized by UV light (30 min) before use. Aquil

160 medium was prepared according to Price et al. (1989) where Synthetic Ocean Water (SOW) is
161 passed through a column containing a Chelex 100 resin (Bio-Rad) in order to remove all trace
162 metals including Fe (Davey *et al.* 1970). Carbon sources were chelexed separately to form
163 stock solutions of 3 M[C] and were added to the medium as single carbon sources (6 mM[C]
164 final concentration). SOW was filtered (0.2 µm) and further sterilized by microwaving it 3
165 times at 750 W until boiling before the addition of nutrients, vitamins and metals all filtered
166 through a 0.2 µm syringe Acrodisc filter (Pall Corporation). Fe-concentrations in the medium
167 were derived from a stock solution of $FeCl_3$ complexed with EDTA at a 1:1 ratio for at least
168 24 h before being subsequently filtered (0.2 µm) and added to the Aquil medium (5.4 µM final
169 concentration).

170

171 Bacteria were grown in 30 mL Thermo Scientific™ Nalgene™ polycarbonate bottles with 12
172 mL of Aquil medium containing 6 mM[C] glucose and transferred into fresh growth medium
173 every 2 days with a starting dilution of approximately 1.8×10^4 cells mL^{-1}. When Fe-
174 contamination could not be accounted for, which occurred when using medium containing Cm
175 or luciferin, the addition of 50 µM of the strong Fe-chelator Desferroxamine-B (DFOB) was
176 used to obtain Fe-deplete conditions in *P. angustum* S14. An overview of all the conducted
177 experiments and their aim can be seen in Table 1.

178 **2.4. Ptr-luc PR gene expression experiments**

179 The bioreporter ptr-luc was used to measure the gene expression of PR over time via
180 luminescence (arbitrary units, a.u.) under various different conditions. Ptr-luc was grown under
181 different wavelengths of red (570-638 nm), green (485-570 nm) and blue light (434-502 nm),
182 and light intensities (0, 15, 30, 60 µmol quanta m^{-2} s^{-1}) using light-emitting diodes (LEDs)
183 coupled to a ventilation system to regulate temperature, and grown under different single

carbon sources (acetate, glucose, serine) in varying concentrations (60, 600, 6000 µM[C]). Fe-deplete conditions were obtained through the addition of 50 µM DFOB.

Luminescence was measured every hour (5 s per well) using an automated microplate luminometer (Berthold LB Centro LB; Thommen *et al.* 2015). The obtained luminescence measurements were corrected for by subtracting the observed background noise derived from the blanks (Supplementary Fig 2) from the sample measurements. In order to obtain a luminescence signal with a high enough resolution for the observation of possible changes during the start of the experiment, ptr-luc was diluted in Aquil media to a starting concentration of ~1.0 x 10^6 cells mL^{-1}. 200µL of the culture was pipetted into each well of a clear-bottom black 96-well microplate (Greiner Bio-One) containing luciferin (final concentration 250 µM) and covered with a clear diamond film seal (Thermo Fisher Scientific™). Bacterial cell counts were performed on samples fixed with formaldehyde (0.2% final concentrations) and stained with SYBR Green I (15 min) using a Becton Dickinson Accuri C6 flow cytometer (Marie *et al.* 1997).

2.5. Wt and Δpr experiments

In order to address the question of how PR gene expression can affect growth under different light and Fe regimes, comparative experiments were conducted between the *P. angustum* S14 wildtype (wt) and Δpr. The strains were grown at a starting abundance of ~1.8 × x10^5 cells mL^{-1} in a range of blue light (LEDs; 434-502 nm range) intensities (0, 15, 30 and 60 µmol quanta m^{-2} s^{-1}) and Fe concentrations (5.4 µM, 0.54 µM, 54 nM, 5.4 nM).

For the construction of bacterial growth curves, cell counts were performed as described above. In parallel, the mean cell volume ($µm^3$) was determined for several time points using a coulter

counter (CASY Cell Counter, Roche) with a 45 µm capillary and a cellular size range between 0.7 and 30 µm and analyzed according to the manufacturer's instructions. The mean volume was calculated from the measured particles within each sample (>0.7 µm).

Respiration rates and growth rates of wt and Δpr were obtained from O_2 measurements conducted using a SensorDish reader (Presens) equipped with 24 glass vials of 4.8 mL containing non-invasive O_2 sensors (OxoDish) and placed in an incubator at a constant temperature of 20°C for a period of 24 hours as described previously (Koedooder et al., 2018; Supplementary Text).

ATP measurements (fmol per 1000 cells) were taken from wt subjected to Fe-replete and Fe-deplete (50 µM DFOB) conditions using the ATP Biomass Kit HS (BioThema) by a luminometer and following the manufacturer's instructions (Lundin, 2000).

The presence of reactive oxygen species (ROS) from ptr-luc was measured using the CellROX® Deep Red reagent according to the manufacturer's instructions (Lifetechnologies, Switzerland) in bacterial cells (Manoil and Bouillaguet 2018). Briefly, CellROX® Deep Red is a cell permeable dye that detects oxidative stress in cells by reacting to ROS in the cells and becoming brightly fluorescent upon oxidation (excitation/emission of 640/665 nm). Ptr-luc was grown in their respective media and pipetted into 200 µL wells of a clear-bottom 96-well microplate (Greiner Bio-One) and covered with a clear diamond film seal (Thermo Fisher Scientific™). Cells were incubated for 30 minutes with 5 µM CellROX® Deep Red and then consequently fixed with formaldehyde (0.2% final concentration) and stained with SYBR Green I (15 min). Fluorescence from CellROX® Deep Red was measured from the

allophycocyanin (APC)-H channel using a BD FACS-Canto II. The geometric mean was taken and expressed in relative fluorescence units (rfu).

2.6. Statistical Analysis

All statistical analyses were conducted in R software (Version 3.5.1) and consisted of a one-way or two-way Analysis of Variance (ANOVA) once the assumptions of normality (Shapiro-Wilk) and homogeneity of variance (Levene Test) were met. A Tukey HSD test was conducted to further elucidate significant interactive results amongst the different conditions[*].

3. Results

3.1. PR gene expression patterns in *P. angustum* S14

The PR gene expression pattern in *P. angustum* S14 was determined under different growth conditions using the luminescent bioreporter ptr-luc (Table 1). In order to determine whether PR gene expression was stimulated by a certain wavelength of light, ptr-luc was subjected to continuous dark, red, green and blue light conditions (30 µmol quanta m^{-2} s^{-1}) and the total luminescence was observed over time (Figure 1). A sudden increase in luminescence was observed in both the dark and all light conditions after 8h of incubation. The luminescence continues to increase thereafter in blue light but not in the other light conditions, which indicates that *P. angustum* S14 specifically induces its PR gene under blue light but not under red or green light or in the dark.

Ptr-luc was further subjected to 12-hour light:12-hour dark or 12-hour dark:12-hour light cycles in order to test how sensitive PR gene expression was to the presence or absence of blue light

[*] The outcome of all statistical analyses has been deposited under the following github link: https://github.com/cocokoedooder/STATS_PRP.angS14

(Supplementary Fig 3). As shown previously, an increase in luminescence was observed in all conditions after 8-hours, followed by a further increase of luminescence over time in the presence of blue light that was absent under dark conditions. Importantly, after ~24 hours, PR gene expression was stimulated by the presence of blue light and turning off or turning on the light respectively resulted in a decrease or increase of the luminescent signal.

When normalizing the total luminescence by cell counts (Figure 2), ptr-luc grown under Fe-replete conditions and continuous blue light, was shown to express a low luminescent signal within the exponential growth phase. Upon approaching the stationary phase at around ~30 hours, the luminescence signal increased per cell in both light and dark conditions. The increased luminescent signal became significantly higher in the presence of blue light compared to the dark at ~48 hours ($p=0.0006$) and ~57 hours ($p<0.0001$). Luminescence peaked around ~60 hours and then gradually declined over time in both light and dark conditions. When comparing the growth rates of ptr-luc grown in Fe-replete conditions in the presence (7.4 ± 0.1 day^{-1}) or absence (7.1 ± 0.4 day^{-1}) of blue light (Table 2), no significant differences were observed ($p=0.9081$). The growth rates further coincided with a maximum cell abundance of $1.31 \pm 0.29 \times 10^8$ cells per mL in the presence and $1.26 \pm 0.09 \times 10^8$ cells per mL in the absence of blue light and was not found to be statistically different ($p=0.2345$).

In order to test whether the gene expression pattern of PR could be affected by the carbon concentration in the medium, ptr-luc was grown in a range of glucose concentrations (60, 600 6000 μM[C]) in the presence and absence of light (Supplementary Fig 4). The gene expression pattern that was observed previously under Fe-replete conditions became less distinct. Specifically, the clear distinction in PR gene expression between light and dark conditions

280 became less pronounced in lower carbon concentrations (600 μM[C]) and was absent in the
281 lowest carbon concentration (60 μM[C]).

282

283 Ptr-luc was further grown under Fe-limiting conditions (50 μM DFOB) in order to see if the
284 gene expression pattern of PR would change compared to Fe-replete conditions. Growth rates
285 respectively declined to 4.0 ± 0.1 and 5.1 ± 1.0 (day^{-1}) in the presence or absence of light (Table
286 2), but again were not found to be significantly different (p=0.1451). The decline in growth
287 rate respectively coincided with a decline in maximum cell abundance to 0.11 ± 0.08 and 0.11
288 ± 0.13 x 10^8 cells per mL in dark or blue light conditions which was not significantly different
289 (p=0.9948). When looking at the total luminescence normalized by cell counts, the gene
290 expression experiments again revealed that as ptr-luc approached the stationary phase at ~20
291 hours, an increase in luminescence was observed in both light and dark conditions (Figure 3).
292 Unlike what was observed for Fe-replete conditions, under Fe-limitation, no significant
293 differences in the luminescence per cell was found between light and dark conditions
294 (p=0.8866).

295

296 Lastly, in order to determine whether single-carbon sources other than glucose could change
297 the PR gene expression pattern in *P. angustum* S14, ptr-luc was grown in either 6mM[C]
298 acetate or 6mM[C] serine in the presence of blue light (Supplementary Fig 5). Compared to
299 glucose, a lower luminescence signal was observed in serine while the signal completely
300 flatlined in the presence of acetate (Supplementary Fig 5). For cells grown in acetate, the low
301 luminescent signal in the presence of light, was due to the absence of cell growth. Under further
302 investigation, the presence of light for cells grown in acetate was coupled to a significantly
303 higher presence of reactive oxygen species (ROS) which doubled in the presence of blue light
304 in comparison to cells grown in the dark (Supplementary Table 2).

3.2. Comparison between the wt and Δpr

Growth experiments of wt and Δpr in a range of Fe and light concentrations allowed us to establish the effect of a well-defined Fe-concentration gradient regarding growth rates and total cell abundance (Supplementary Fig 6, Table 1). Overall, decreasing Fe-concentrations resulted in a significant and gradual decline in both the growth rate ($p<0.0001$) and maximum cell abundance ($p<0.0001$) of both wt (Supplementary Table 3) and Δpr (Supplementary Table 4).

In Fe-replete conditions (5.4 µM), the growth rates and maximum cell abundance of wt were similar to what was obtained for ptr-luc, reaching values between 7.1 ± 0.1 and 7.4 ± 0.1 (day^{-1}) and 1.4 ± 0.1 and 1.1 ± 0.1 x 10^8 cells per mL respectively. These values decreased with lower Fe-concentrations to growth rates between 3.8 ± 0.1 and 4.3 ± 0.2 (day^{-1}) and maximum cell abundances between 0.2 ± 0.1 and 0.3 ± 0.1 x 10^8 cells per mL) under 5.4 nM Fe, respectively. Furthermore, the maximum cell abundance obtained from wt grown under 5.4 µM and 0.54 µM of Fe was similar to each other, indicating that, at these concentrations, Fe is not considered to be a limiting factor within the medium and that at 5.4 µM Fe is in excess. Fe-limitation caused a similar decline in both the growth rate ($p<0.0001$) and maximum cell abundance ($p<0.0001$) in Δpr (Supplementary Figure 6; Supplementary Table 4).

The presence of light significantly affected both the growth rate ($p=0.0004$) and maximum cell abundance ($p=0.0007$) of wt (Figure 4, Supplementary Table 3). Under 5.4 nM of Fe, a small but significantly lower growth rate was observed in the dark compared to 25, 50 and 100% blue light. The opposite response was observed in Fe-replete conditions (5.4 µM) where a small but higher growth rate was observed in the dark compared to the light treatments. Under high

light intensities, significantly lower maximum cell abundances were observed for wt grown in 5.4 µM of Fe ($p=0.0013$). Similar results were obtained from growth experiments conducted on Δpr. A significant interactive effect between light and Fe-concentrations occurred on both the growth rate ($p=0.0001$) and maximum cell abundance ($p=0.0029$) (Supplementary Table 4). A Tukey Test revealed that under Fe-replete conditions, no negative effect of light was observed on the growth of Δpr under high light intensities (100% blue light) as was previously shown for wt. Similar to wt, under Fe-limiting conditions an increase in the maximum cell abundance was observed under high light intensities and under 54 nM a significant increase in the growth rate was observed ($p=0.0022$).

Growth and respiration rates derived from O_2 measurements were taken for both the wt and Δpr grown under Fe-limiting conditions (100 µM DFOB) in the presence and absence of light (Table 3). In the presence of light, no significant differences were observed in the respiration rate ($p=0.999$). Significant differences in the growth rate between the wt and Δpr ($p=0.045$) were observed but concerned a respectively small difference of 0.2 (2.6 ± 0.1 and 2.8 ± 0.05 day^{-1}).

Changes in cell volume were measured for wt grown in both Fe-replete (5.4µM) and Fe-limiting (50µM DFOB) conditions in the presence or absence of light over time (Figure 5, Supplementary Table 5). Cell volumes were always slightly lower in constant blue light compared to dark-conditions. The mean cell volume declined over time from 1.44 ± 0.01 μm^3 and 1.35 ± 0.01 μm^3 in Fe-limiting and Fe-replete conditions to 0.76 ± 0.01 μm^3 and 0.69 ± 0.01 μm^3 respectively.

Lastly, ATP measurements were taken for wt grown in Fe-replete (5.4μM) and Fe-limiting (50μM DFOB) conditions that coincided with cells entering the stationary phase (Table 4). ATP measurements were significantly lower in Fe-limiting conditions compared to Fe-replete conditions, but no significant differences were observed in the presence or absence of light under both Fe-conditions.

4. Discussion

4.1. PR gene expression pattern of *P. angustum* S14 is linked to a starvation state

The gene expression pattern of PR is known to differ amongst various bacterial strains as several studies have been able to demonstrate that the PR gene can be either facultatively or continuously expressed within the cell (Supplementary Table 1). Our results established that *P. angustum* S14 facultatively expresses its PR gene as cells approach the stationary phase and that this occurs in both Fe-replete and Fe-limiting conditions. The gene expression pattern of PR in *P. angustum* S14 was similar to other members of the Vibrionaceae family including *Vibrio sp.* AND4 and *Vibrio campbelli*, both of which contain green-tuned PR molecules (Gómez-Consarnau *et al.* 2010; Wang *et al.* 2012; Akram *et al.* 2013). Due to the presence of glutamine in position 105 of its amino acid sequence, the PR present in *P. angustum* S14 is expected to be tuned towards blue light which coincides with our results. Thus far, *P. angustum* S14 is the only known bacterial strain in culture containing a blue-tuned PR molecule of which the PR gene expression pattern has been elucidated.

In the stationary phase, significant differences in the PR gene expression of *P. angustum* S14 were observed in the presence and absence of light and these differences only became apparent under high glucose concentrations of 600 μM[C] and 6mM[C] but not 60 μM[C]. For other

members of the Vibrionaceae family, significant differences in the PR gene expression in the presence or absence of light have been observed in *V. campbelli* (132 μM[C]; Wang et al., 2012), but not for *Vibrio* sp. AND4 (2 mM[C]; Akram et al., 2013). While it is important to note that the two experiments are not strictly comparable due to differences in their culture media and carbon source, the carbon concentration present within the medium can be relevant in these expression analyses. In *Dokdonia sp.* MED 134 (Gómez-Consarnau *et al.* 2007), for example, significant differences in the gene expression of PR in the presence or absence of light only appeared under DOC concentrations ranging between 140 μM[C] and 1.1 mM[C] but not in lower (60 μM[C]) or higher (242 mM[C]) carbon concentrations. Unlike members of the Vibrionaceae family, however, *Dokdonia sp.* MED 134 has been shown to constitutively express PR in the presence of light (Palovaara *et al.* 2014; Gómez-Consarnau *et al.* 2016).

As cells approached the stationary phase, the increased gene expression of PR was coupled with a strong decrease in cellular biovolume over time under both Fe-replete and Fe-limiting conditions. The ability to starkly reduce cellular biovolume is a characteristic trait that occurs when cells are capable of inducing a stringently controlled starvation state upon energy and carbon deprivation (Kjelleberg, Humphrey and Marshall 1982; Nyström and Kjelleberg 1989; Nyström, Olsson and Kjelleberg 1992). The induction of a starvation state is a phenomenon commonly observed in several members of the Vibrionaceae family including *P. angustum* S14 (Hild *et al.* 2000; Lauro *et al.* 2009; Lever *et al.* 2015). The gene expression pattern of PR in both *V. campbelli* and *Vibrio sp*. AND4 has previously been linked to the alternative sigma factor RpoS1 which instigates the induction of a starvation state (Wang *et al.* 2012; Akram *et al.* 2013). It is therefore likely that a similar form of regulation may be occurring in *P. angustum* S14 under both carbon-limitation and Fe-limitation.

Previous experiments have shown that the reduction in cellular biovolume observed in *P. angustum* S14 is absent under other forms of limitation such as low phosphorus and nitrogen concentrations (Holmquist and Kjelleberg 1993). Our results, hereby, indicate that Fe-limitation, like carbon limitation, induces a starvation-like state in *P. angustum* S14. The lower biovolume observed in the presence of Fe-limitation was in contrast to what was shown for *E. coli* (Hubbard *et al.* 1986) and a small oceanic *A. macleodii* strain (Fourquez *et al.* 2014), the latter of which resulted in a 2-fold increase in its biovolume under Fe-limiting conditions. While carbon-limitation will directly affect energy production within the cell and is known from previous studies to induce a starvation state in *P. angustum* S14 (Holmquist and Kjelleberg 1993), the effect of Fe-limitation on the energy status of the cell is inherently more complex. Fe-limitation is known to indirectly affect energy production within the cell by affecting the synthesis of Fe-containing enzymes. These include enzymes located within the respiratory electron transport chain, and enzymes involved in the TCA cycle and DNA synthesis (Tortell, Maldonado and Price 1996).

A large fraction of the heterotrophic bacteria are considered to be present in a starvation-like state until specific nutrients become available for them to grow (Burgess 1997; Gray *et al.* 2019) and, for members of the Vibrionaceae family, PR is currently considered to be an important mechanism to maintain sufficient energy-levels to keep basal metabolic functioning within the cell under unfavourable and starved conditions (Gómez-Consarnau *et al.* 2010; Akram *et al.* 2013). Extended growth experiments conducted for both wt and Δpr in the presence or absence of light also did not result in any further significant differences which is in contrast to what was observed in *Vibrio sp*. AND4 where an enhanced survival upon starvation conditions occurred by means of a series of dilution experiments (Gómez-Consarnau *et al.* 2010; Akram *et al.* 2013). The effect of light on *P. angustum* S14 in the context of

maintenance energy and carbon yield had previously been studied using continuous culture experiments (Courties *et al.* 2015). When correcting for variations in the dilution rates, Courties *et al* (2015) reported an increase in the carbon yield for cells subjected to light and dark cycles compared to dark controls. It was predicted that higher carbon yields resulted from a lower maintenance coefficient that could be attributed to PR activity although PR gene expression had not been measured in these experiments. As continuous culture experiments aim to target the exponential growth phase, these predictions were in contrast to our finding that PR activity in *P. angustum* S14 specifically occurs as cells enter the stationary phase and appears to be linked to a starvation-like state.

4.2. PR gene expression pattern of *P. angustum* S14 grown in alanine and serine

Experiments conducted by Palovaara *et al* (2014) for *Dokdonia* sp. MED 134 compared the effect of PR under different single carbon sources. Growth of *Dokdonia* sp. MED 134 under a "poor" carbon source such as alanine resulted in a stronger difference in the enhanced bacterial growth- and uptake rates in the presence of light when compared to glucose. In previous experiments, *P. angustum* S14 has been shown to grow on "poor" carbon sources such as serine and acetate (Koedooder *et al.* 2018). When *P. angustum* S14 was grown under carbon sources other than glucose, such as serine and acetate, we hereby predicted that any affect from PR activity in the presence of light may be enhanced. Instead, growth under acetate or serine was hindered in the presence of light and appeared to heighten the susceptibility of *P. angustum* S14 towards photo-oxidative stress as a significant build-up of ROS was observed within the cell that increased in the presence of light. It is well established that the various methods in which a bacterial strain can combat (photo)oxidative stress are strain specific (Cabiscol, Tamarit and Ros 2000). *P. angustum* S14 is particularly known to contain a wide diversity of pathways to counter oxidative stress (Matallana-Surget *et al.* 2012, 2013). Our results

emphasize that the sensitivity of ptr-luc grown in acetate and serine towards continuous blue light ultimately outweighed any potential benefit for the cells in terms of PR activity.

4.3. PR gene expression pattern of *P. angustum* S14 in Fe-limitation

In *P. angustum* S14, the PR gene expression was shown to increase over time in the presence of both light and dark conditions under Fe-limitation. This is in line with experiments conducted by Marchetti *et al* (2015) which showed that the presence of Fe-limitation increased the gene expression of PR in the oceanic diatom *P. granii* compared to Fe-replete conditions. Importantly, Marchetti *et al* (2015) did not link these expression experiments to a particular growth phase and whether the observed increase in PR gene expression in *P. granii* specifically occurs as cells were entering the stationary phase could not be determined from these experiments.

Our results highlight that care must be taken when attributing changes in growth rate and cell yield to the presence of PR within the cell. Under Fe-limitation, a small but significant enhanced growth rate and maximum cell abundance was observed in the presence of light compared to the dark. Based on our expression experiments and on further investigation using Δpr, the enhanced growth rate and maximum cell abundance was not due to the presence of PR in *P. angustum* S14. Instead, it is likely due to an enhanced bioavailability of Fe through the photo-reduction of the Fe:EDTA complex within the medium (Sunda and Huntsman 2003; Barbeau 2006). In contrast, under Fe-replete conditions, the presence of light resulted in a slightly lower growth rate and maximum cell abundance which may be attributed to an enhancement of photo-oxidative stress by means of the Fenton reaction (Touati 2000; Dixon and Stockwell 2014; Mullarky and Cantley 2015). Similar growth rates and maximum cell

476 abundances were, for example, obtained for *P. angustum* S14 grown in the presence of both
477 5.4 μM and 0.54 μM of Fe and is an indication that *P. angustum* S14 is grown under Fe-excess.
478 Furthermore, while Fe-limitation clearly reduced ATP concentrations and respiration rates
479 within the cell, no significant differences were observed in *P. angustum* S14 in the presence or
480 absence of light. Similarly, the experiments conducted with *P. granii* did not result in additional
481 differences in the growth rate or maximum cell abundances (Marchetti *et al.* 2015).

482

483 In conclusion, our results contribute to the growing body of PR gene expression studies that
484 have been conducted over the past decade. While our observations strengthen the finding that
485 PR seems to play an important role within the stationary phase for several members of the
486 Vibrionaceae family, the exact role of PR, and in particular under Fe-limitation, still remains
487 unclear. Another potential mechanism by which PR can aid a cell within the stationary phase
488 is in the search and uptake of available nutrients. Copiotrophs are often characterized by a wide
489 diversity in transporters that enables the uptake of various nutrients (Ho, Lonardo and Bodelier
490 2017). Under carbon starvation, *P. angustum* S14 has the ability, for example, to induce a high-
491 affinity uptake system for glucose (Lauro *et al.* 2009; Lever *et al.* 2015) and has also been
492 shown to evoke a chemotaxis response towards several carbon sources (Malmcrona-Friberg,
493 Goodman and Kjelleberg 1990). Both the observed chemotaxis response towards glucose in
494 the presence of carbon-starvation and the ability of *P. angustum* S14 to upregulate high-uptake
495 mechanisms for glucose are all potential physiological functions that could ultimately require
496 the use of PR activity and remains to be further elucidated (Fuhrman, Schwalbach and Stingl
497 2008; Gómez-Consarnau *et al.* 2016).

498

499 **5. Funding**

500 This work was financially supported in part by a grant from the French National Research
501 Agency (ANR-16-CE32-0008-01) and the National Center for Marine Biological Resources
502 (EMBRC).

503

504 **6. Acknowledgments**

505 The authors would like to thank Frederique Le Roux and Astrid Lemire for the construction
506 of the gene knockout Δpr and we further wish to acknowledge Valerie Vergé for helping us
507 provide PCR results during the experiments to confirm the absence of PR in the gene
508 knockout Δpr and the presence of the PR-luciferin construct in the bioreporter ptr-luc.
509 Phillipe Catalan for providing guidance with the ROS experiments.

510 **Conflicts of interest.** There are no conflicts of interest to declare.

511

512 **References**

513 Akram N, Palovaara J, Forsberg J *et al.* Regulation of proteorhodopsin gene expression by
514 nutrient limitation in the marine bacterium *Vibrio* sp. AND4. *Environ Microbiol*
515 2013;**15**:1400–15.

516 Alberts B, Johnson A, Lewis J et al. Electron transport chains and their proton pumps. *Mol*
517 *Biol cell 4th Ed* 2002:1–10.

518 Almaas E, Oltvai ZN, Barabási A-L. The Activity Reaction Core and Plasticity of Metabolic
519 Networks. *PLoS Comput Biol* 2005;**1**:e68.

520 Andrews SC, Robinson AK, Rodríguez-Quiñones F. Bacterial iron homeostasis. *FEMS*
521 *Microbiol Rev* 2003;**27**:215–7.

522 Azam. F., Fenchel T, Field JG *et al.* The Ecological Role of Water-Column Microbes in the

523 Sea*. *Ecol Prog Ser, Mar* 1983;**10**:257–63.

524 Barbeau K. Photochemistry of Organic Iron(III) Complexing Ligands in Oceanic Systems.
525 *Photochem Photobiol* 2006;**82**:1505–16.

526 Béjà O, Aravind L, Koonin E V *et al.* Bacterial rhodopsin: evidence for a new type of
527 phototrophy in the sea. *Science* 2000;**289**:1902–6.

528 Béjà O, Spudich EN, Spudich JL *et al.* Proteorhodopsin phototrophy in the ocean. *Nature*
529 2001;**411**:786–9.

530 Bertani G. Studies on lysogenesis. I. The mode of phage liberation by lysogenic Escherichia
531 coli. *J Bacteriol* 1951;**62**:293–300.

532 Blain S, Tagliabue A. *Iron Cycle in Oceans*. Tregeur P (ed.). London: ISTE Ltd and John
533 Wiley & Sons, Inc., 2016.

534 Blankenship RE. Early Evolution of Photosynthesis. *Plant Physiol* 2010;**154**:434–8.

535 Burgess G. Bacteria in Oligotrophic Environments: Starvation Survival Lifestyle. *World J*
536 *Microbiol Biotechnol* 1997;**14**:305–305.

537 Burr DJ, Martin A, Maas EW *et al.* In situ light responses of the proteorhodopsin-bearing
538 Antarctic sea-ice bacterium, Psychroflexus torques. *ISME J* 2017;**11**:2155–8.

539 Cabiscol E, Tamarit J, Ros J. Oxidative stress in bacteria and protein damage by reactive
540 oxygen species. *Int Microbiol* 2000;**3**:3–8.

541 Cohen NR, Gong W, Moran DM *et al.* Transcriptomic and proteomic responses of the
542 oceanic diatom *Pseudo-nitzschia granii* to iron limitation. *Environ Microbiol*
543 2018;**20**:3109–26.

544 Courties A, Riedel T, Rapaport A *et al.* Light-driven increase in carbon yield is linked to
545 maintenance in the proteorhodopsin-containing Photobacterium angustum S14. *Front*

546 *Microbiol* 2015;**6**:688.

547 Davey EW, Gentile JH, Erickson SJ *et al.* Removal of Trace Metals from Marine Cluster
548 Media. *Limnol Oceanogr* 1970;**15**:486–8.

549 Dixon SJ, Stockwell BR. The role of iron and reactive oxygen species in cell death. *Nat*
550 *Chem Biol* 2014;**10**:9–17.

551 Feng S, Powell SM, Wilson R *et al.* Light-stimulated growth of proteorhodopsin-bearing sea-
552 ice psychrophile Psychroflexus torquis is salinity dependent. *ISME J* 2013;**7**:2206–13.

553 Feng S, Powell SM, Wilson R *et al.* Extensive gene acquisition in the extremely
554 psychrophilic bacterial species Psychroflexus torquis and the link to sea-ice ecosystem
555 specialism. *Genome Biol Evol* 2014;**6**:133–48.

556 Feng S, Powell SM, Wilson R *et al.* Proteomic Insight into Functional Changes of
557 Proteorhodopsin-Containing Bacterial Species *Psychroflexus torquis* under Different
558 Illumination and Salinity Levels. *J Proteome Res* 2015;**14**:3848–58.

559 Fourquez M, Devez A, Schaumann A *et al.* Effects of iron limitation on growth and carbon
560 metabolism in oceanic and coastal heterotrophic bacteria. *Limnol Oceanogr*
561 2014;**59**:349–60.

562 Fuhrman JA, Schwalbach MS, Stingl U. Proteorhodopsins: an array of physiological roles?
563 *Nat Rev Microbiol* 2008;**6**:488–94.

564 Giovannoni SJ, Bibbs L, Cho J-C *et al.* Proteorhodopsin in the ubiquitous marine bacterium
565 SAR11. *Nature* 2005;**438**:82–5.

566 Gómez-Consarnau L, Akram N, Lindell K *et al.* Proteorhodopsin Phototrophy Promotes
567 Survival of Marine Bacteria during Starvation. Eisen JA (ed.). *PLoS Biol*
568 2010;**8**:e1000358.

569 Gómez-Consarnau L, González JM, Coll-Lladó M *et al.* Light stimulates growth of
570 proteorhodopsin-containing marine Flavobacteria. *Nature* 2007;**445**:210–3.

571 Gómez-Consarnau L, González JM, Riedel T *et al.* Proteorhodopsin light-enhanced growth
572 linked to vitamin-B1 acquisition in marine Flavobacteria. *ISME J* 2016;**10**:1102–12.

573 Gómez-Consarnau L, Raven JA, Levine NM *et al.* Microbial rhodopsins are major
574 contributors to the solar energy captured in the sea. *Sci Adv* 2019;**5**:eaaw8855.

575 González JM, Fernández-Gómez B, Fernàndez-Guerra A *et al.* Genome analysis of the
576 proteorhodopsin-containing marine bacterium Polaribacter sp. MED152 (Flavobacteria).
577 *Proc Natl Acad Sci U S A* 2008;**105**:8724–9.

578 Gray DA, Dugar G, Gamba P *et al.* Extreme slow growth as alternative strategy to survive
579 deep starvation in bacteria. *Nat Commun* 2019;**10**:890.

580 Hild E, Takayama K, Olsson RM *et al.* Evidence for a role of rpoE in stressed and unstressed
581 cells of marine Vibrio angustum strain S14. *J Bacteriol* 2000;**182**:6964–74.

582 Ho A, Lonardo DP Di, Bodelier PLE. Revisiting life strategy concepts in environmental
583 microbial ecology. *FEMS Microbiol Ecol* 2017;**93**:fix006.

584 Holmquist L, Kjelleberg S. Changes in viability, respiratory activity and morphology of the
585 marine Vibrio sp. strain S14 during starvation of individual nutrients and subsequent
586 recovery. *FEMS Microbiol Ecol* 1993;**12**:215–23.

587 Holms H. Flux analysis and control of the central metabolic pathways in Escherichia coli.
588 *FEMS Microbiol Rev* 1996;**19**:85–116.

589 Hubbard JAM, Lewandowska KB, Hughes MN *et al.* Effects of iron-limitation of Escherichia
590 coli on growth, the respiratory chains and gallium uptake. *Arch Microbiol* 1986;**146**:80–
591 6.

592 Ilbert M, Bonnefoy V. Insight into the evolution of the iron oxidation pathways. *Biochim*
593 *Biophys Acta - Bioenerg* 2013;**1827**:161–75.

594 Kimura H, Young CR, Martinez A *et al.* Light-induced transcriptional responses associated
595 with proteorhodopsin-enhanced growth in a marine flavobacterium. *ISME J*
596 2011;**5**:1641–51.

597 Kirchman DL, Hanson TE. Bioenergetics of photoheterotrophic bacteria in the oceans.
598 *Environ Microbiol Rep* 2013;**5**:188–99.

599 Kjelleberg S, Humphrey BA, Marshall KC. Effect of interfaces on small, starved marine
600 bacteria. *Appl Environ Microbiol* 1982;**43**:1166–72.

601 Koedooder C, Guéneuguès A, Van Geersdaële R *et al.* The Role of the Glyoxylate Shunt in
602 the Acclimation to Iron Limitation in Marine Heterotrophic Bacteria. *Front Mar Sci*
603 2018;**5**, DOI: 10.3389/fmars.2018.00435.

604 Lauro FM, McDougald D, Thomas T *et al.* The genomic basis of trophic strategy in marine
605 bacteria. *Proc Natl Acad Sci U S A* 2009;**106**:15527–33.

606 Lemire A, Goudenège D, Versigny T *et al.* Populations, not clones, are the unit of vibrio
607 pathogenesis in naturally infected oysters. *ISME J* 2015;**9**:1523–31.

608 Lever MA, Rogers KL, Lloyd KG *et al.* Life under extreme energy limitation: a synthesis of
609 laboratory- and field-based investigations. Giudici-Orticoni M-T (ed.). *FEMS Microbiol*
610 *Rev* 2015;**39**:688–728.

611 Lis H, Shaked Y, Kranzler C *et al.* Iron bioavailability to phytoplankton: an empirical
612 approach. *ISME J* 2015;**9**:1003–13.

613 Malmcrona-Friberg K, Goodman A, Kjelleberg S. Chemotactic Responses of Marine Vibrio
614 sp. Strain S14 (CCUG 15956) to Low-Molecular-Weight Substances under Starvation

615 and Recovery Conditions. *Appl Environ Microbiol* 1990;**56**:3699–704.

616 Manoil D, Bouillaguet S. Oxidative Stress in Bacteria Measured by Flow Cytometry. 2018;**6**,
617 DOI: 10.19080/AIBM.2018.08.555726.

618 Marchetti A, Catlett D, Hopkinson BM *et al.* Marine diatom proteorhodopsins and their
619 potential role in coping with low iron availability. *ISME J* 2015;**9**:2745–8.

620 Marchetti A, Schruth DM, Durkin CA *et al.* Comparative metatranscriptomics identifies
621 molecular bases for the physiological responses of phytoplankton to varying iron
622 availability. *Proc Natl Acad Sci* 2012;**109**:E317–25.

623 Marie D, Partensky F, Jacquet S *et al.* Enumeration and Cell Cycle Analysis of Natural
624 Populations of Marine Picoplankton by Flow Cytometry Using the Nucleic Acid Stain
625 SYBR Green I. *Appl Environ Microbiol* 1997;**63**:186–93.

626 Martinez A, Bradley AS, Waldbauer JR *et al.* Proteorhodopsin photosystem gene expression
627 enables photophosphorylation in a heterologous host. *Proc Natl Acad Sci U S A*
628 2007;**104**:5590–5.

629 Matallana-Surget S, Cavicchioli R, Fauconnier C *et al.* Shotgun Redox Proteomics:
630 Identification and Quantitation of Carbonylated Proteins in the UVB-Resistant Marine
631 Bacterium, Photobacterium angustum S14. Gasset M (ed.). *PLoS One* 2013;**8**:e68112.

632 Matallana-Surget S, Joux F, Wattiez R *et al.* Proteome Analysis of the UVB-Resistant
633 Marine Bacterium Photobacterium angustum S14. Gasset M (ed.). *PLoS One*
634 2012;**7**:e42299.

635 Merchant SS, Helmann JD. Elemental Economy: Microbial Strategies for Optimizing Growth
636 in the Face of Nutrient Limitation. *Adv Microb Physiol* 2012;**60**:91–210.

637 Morel FMM, Rueter JG, Anderson DM *et al.* Aquil: A chemically definied phytoplankton

638 culture medium for trace metal studies. *J Phycol* 2008;**15**:135–41.

639 Mullarky E, Cantley LC. Diverting Glycolysis to Combat Oxidative Stress. In: Nakao,
640 Kazuwa; Minato, Nagahiro; Uemoto S (ed.). *Innovative Medicine: Basic Research and*
641 *Development*. Tokyo: Springer, 2015, 3–23.

642 Nyström T, Kjelleberg S. Role of Protein Synthesis in the Cell Division and Starvation
643 Induced Resistance to Autolysis of a Marine Vibrio during the Initial Phase of
644 Starvation. *Microbiology* 1989;**135**:1599–606.

645 Nyström T, Olsson RM, Kjelleberg S. Survival, stress resistance, and alterations in protein
646 expression in the marine vibrio sp. strain S14 during starvation for different individual
647 nutrients. *Appl Environ Microbiol* 1992;**58**:55–65.

648 Oppenheimer H. C., ZoBell C. The growth and viability of sixty-three species of marine
649 bacteria as influenced by hydrostatic pressure. *J Mar Res* 1952;**11**:10–8.

650 Palovaara J, Akram N, Baltar F *et al.* Stimulation of growth by proteorhodopsin phototrophy
651 involves regulation of central metabolic pathways in marine planktonic bacteria. *PNAS*
652 2014;**111**:e3650–8.

653 Pinhassi J, DeLong EF, Béjà O *et al.* Marine Bacterial and Archaeal Ion-Pumping
654 Rhodopsins: Genetic Diversity, Physiology, and Ecology. *Microbiol Mol Biol Rev*
655 2016;**80**:929–54.

656 Price N, Harrison G, Hering J *et al.* Preparation and Chemistry of the Artificial Algal Culture
657 Medium Aquil. *Biol Oceanogr* 1989;**6**:443–61.

658 Raven JA. Functional evolution of photochemical energy transformations in oxygen-
659 producing organisms. *Funct Plant Biol* 2009;**36**:505–15.

660 Le Roux F, Binesse J, Saulnier D *et al.* Construction of a Vibrio splendidus mutant lacking

661 the metalloprotease gene vsm by use of a novel counterselectable suicide vector. *Appl*
662 *Environ Microbiol* 2007;**73**:777–84.

663 Le Roux F, Davis BM, Waldor MK. Conserved small RNAs govern replication and
664 incompatibility of a diverse new plasmid family from marine bacteria. *Nucleic Acids Res*
665 2011;**39**:1004–13.

666 Song Y, Cartron ML, Jackson PJ *et al.* Overproduction of proteorhodopsin enhances long-
667 term viability of Escherichia coli. *Appl Environ Microbiol* 2020;**86**:e02087-19.

668 Steindler L, Schwalbach MS, Smith DP *et al.* Energy starved Candidatus Pelagibacter ubique
669 substitutes light-mediated ATP production for endogenous carbon respiration. Gilbert
670 JA (ed.). *PLoS One* 2011;**6**:e19725.

671 Stingl U, Tripp HJ, Giovannoni SJ. Improvements of high-throughput culturing yielded novel
672 SAR11 strains and other abundant marine bacteria from the Oregon coast and the
673 Bermuda Atlantic Time Series study site. *ISME J* 2007;**1**:361–71.

674 Sun Y, Zhang Y, Hollibaugh JT *et al.* Ecotype diversification of an abundant Roseobacter
675 lineage. *Environ Microbiol* 2017;**19**:1625–38.

676 Sunda W, Huntsman S. Effect of pH, light, and temperature on Fe–EDTA chelation and Fe
677 hydrolysis in seawater. *Mar Chem* 2003;**84**:35–47.

678 Tagliabue A, Bowie AR, Boyd PW *et al.* The integral role of iron in ocean biogeochemistry.
679 *Nature* 2017;**543**:51–9.

680 Terashima M, Ohashi K, Takasuka TE *et al.* Antarctic heterotrophic bacterium
681 Hymenobacter nivis P3 T displays light-enhanced growth and expresses putative
682 photoactive proteins. *Environ Microbiol Rep* 2019;**11**:227–35.

683 Thommen Q, Pfeuty B, Schatt P *et al.* Probing entrainment of Ostreococcus tauri circadian

clock by green and blue light through a mathematical modeling approach Quentin. *Front Genet* 2015;**6**, DOI: 10.3389/fgene.2015.00065.

Tortell PD, Maldonado MT, Granger J *et al.* Marine bacteria and biogeochemical cycling of iron in the oceans. *FEMS Microbiol Ecol* 1999.

Tortell PD, Maldonado MT, Price NM. The role of heterotrophic bacteria in iron-limited ocean ecosystems. *Nature* 1996;**383**:330–2.

Touati D. Iron and Oxidative Stress in Bacteria. *Arch Biochem Biophys* 2000;**373**:1–6.

Val M-E, Skovgaard O, Ducos-Galand M *et al.* Genome Engineering in Vibrio cholerae: A Feasible Approach to Address Biological Issues. Guttman DS (ed.). *PLoS Genet* 2012;**8**:e1002472.

Wang Z, O'Shaughnessy TJ, Soto CM *et al.* Function and Regulation of Vibrio campbellii Proteorhodopsin: Acquired Phototrophy in a Classical Organoheterotroph. Harvey BK (ed.). *PLoS One* 2012;**7**:e38749.

Yoshizawa S, Kumagai Y, Kim H *et al.* Functional characterization of flavobacteria rhodopsins reveals a unique class of light-driven chloride pump in bacteria. *Proc Natl Acad Sci U S A* 2014;**111**:6732–7.

Lundin A. Use of firefly luciferase in atp-related assays of biomass, enzymes, and metabolites. *Methods Enzymol* 2000;**305**:346–70.

7. Table Legends

Table 1. *Overview and aim of the different experiments performed with the P. angustum S14 wildtype (wt), the PR luminescent bioreporter (ptr-luc) and PR gene knockout (Δpr).*

Table 2. *Growth rates (μ) and maximum cell abundance of ptr-luc grown in Fe-replete and Fe-limiting conditions, in the presence or absence of light.* ***(n=3)***

Table 3. *Growth rates (μ) and cellular respiration rates derived from O_2 measurements of P. angustum S14 (wt) and Δpr grown in Fe-limiting conditions (100 μM DFOB) and the presence of constant light or dark conditions. Statistically significant values are marked in bold.* ***(n=3)***

Table 4. *ATP measurements taken at 20 h (coinciding with the exponential phase) for P. angustum S14 (wt) grown in Fe-replete and Fe-limiting conditions and p-values of a 1-way ANOVA comparing differences between light and dark conditions after a ln transformation in order to meet the assumptions of homogeneity of variance.* ***(n=4)***

8. Figure Legends

Figure 1. *Ptr-luc grown in Aquil medium and 6mM[C] glucose subjected to either (a) no light, (b) red-light, (c) green-light and (d) blue-light. Light intensity for all wavelengths was set at 30 μmol quanta m^{-2} s^{-1}. An increase in luminescence occurs at ~8 hours and continues to increase in blue light but not in the other light conditions.* ***(n=5)***

Figure 2. *Ptr-luc grown in Fe-replete conditions in Aquil medium and 6mM[C] glucose subjected to either dark (dark red circles) or constant blue light (light red circles; 30 μmol quanta m^{-2} s^{-1}). (a) Total luminescence where vertical dashed lines represent the time points when cell counts were taken, (b) cell counts and (c) luminescence per cell. Total luminescence increases after ~25 hours in the presence of both light and dark, which coincides with the time cells are approaching the stationary phase. In the presence of light, luminescence continues to increase and peaks at ~60 hours which coincides with slightly elevated cell counts in the presence of light compared to dark conditions, albeit this is not significantly different.* ***(n=3)***

Figure 3. *Ptr-luc grown in Fe-limiting conditions (50 μM DFOB) in Aquil medium and 6mM[C] glucose subjected to either dark conditions (dark blue circles) or constant blue light (light blue circles; 30 μmol quanta m^{-2} s^{-1}). (a) total luminescence where vertical dashed lines represent the time points when cell counts were taken, (b) cell counts and (c) luminescence per cell. Total luminescence shows an increase in expression after ~20 hours in the presence of both light and dark, which coincides with the time cells are approaching the stationary phase. No clear difference between light and dark conditions were observed.* ***(n=3)***

Figure 4. *The relationship between the growth rate (day^{-1}) of P. angustum S14 (wt) for a range of Fe-concentrations grown in either 0, 25, 50, 100% blue light (dark grey, grey, light grey and white circles) where 100% light was equivalent to 60 μmol quanta m^{-2} s^{-1}. Under low Fe-concentrations (5.4 nM), the presence of light positively influences the growth rate while under high Fe-concentrations (5.4 μM), the presence of light negatively influences the growth rate.* ***(n=3)***

Figure 5. *Mean cell volume (μm^3) of P. angustum S14 (wt) at several time points grown in either 6mM[C] of glucose in Fe-limiting (blue) or Fe-replete (red) conditions and subjected to constant darkness (dark blue or red) or blue light (light blue or light red; 30 μmol quanta m^{-2} s^{-1}). At 1 hour, cell size was measured from acclimated cells grown overnight in glucose and Fe-replete conditions. 24 hours coincides with the end of the exponential growth phase*

and start of the exponential phase. 50 hours coincides with peak proteorhodopsin expression and 75 hours when the expression of proteorhodopsin is in decline. ***(n=3)***

9. Tables

Table 1. *Overview and aim of the different experiments performed with the P. angustum S14 wildtype (wt), the PR luminescent bioreporter (ptr-luc) and PR gene knockout (Δpr).*

Strain	***Fe-regime***	***Carbon***	***Light regime***	***Aim***
PR gene expression Pattern				
ptr-luc	*+Fe*	*glucose*	*dark, red, green, blue*	*PR gene expression in dark, red, green, or blue light*
	+Fe	*glucose*	*dark, 12:12DL, 12:12LD, blue*	*PR gene expression and sensitivity towards switching-on or switching-off the light*
	+Fe, -Fe	*glucose*	*dark, blue*	*PR gene expression under Fe-replete and Fe-limited conditions*
	+Fe	*glucose (gradient)*	*dark, blue*	*PR gene expression under different glucose concentrations*
	+Fe	*acetate, serine*	*dark, blue*	*PR gene expression under different carbon sources*
Comparison between wt and Δpr				
wt, Δpr	*Fe-gradient*	*glucose*	*blue (gradient)*	*Effect of light and Fe on growth rates and cell yield*
wt, Δpr	*-Fe*	*glucose*	*dark, blue*	*Effect of light on growth rates and respiration rates using O_2 measurements*
wt	*+Fe, -Fe*	*glucose*	*dark, blue*	*Effect of light on cell volume*
wt	*+Fe, -Fe*	*glucose*	*dark, blue*	*Effect of light on ATP concentrations*

Table 2. *Growth rates (μ) and maximum cell abundance of ptr-luc grown in Fe-replete and Fe-limiting conditions, in the presence or absence of light.* ***(n=3)***

Conditions	**μ (day^{-1})**	**Bacteria (10^8 cells mL^{-1})**
Fe-rep + dark	7.4 ± 0.1	1.26 ± 0.09
Fe-rep + light	7.1 ± 0.4	1.31 ± 0.29
p-value	p=0.9081	p=0.2345
Fe-lim + dark	4.0 ± 0.1	0.11 ± 0.08
Fe-lim + light	5.1 ± 1.0	0.11 ± 0.13
p-value	p=0.1451	p=0.9948

Table 3. *Growth rates (μ) and cellular respiration rates derived from O_2 measurements of P. angustum S14 (wt) and Δpr grown in Fe-limiting conditions (100 μM DFOB) and the presence of constant light or dark conditions. Statistically significant values are marked in bold.* ***(n=3)***

μ (day^{-1})	**wt**	**Δpr**	**p-value**
light	2.6 ±0.1	2.8 ±0.1	**p=0.045**
dark	2.6 ±0.1	3.0 ±0.2	p=0.108
Respiration rate ($fmol\ cell^{-1}\ h^{-1}$)			
light	0.08 ±0.02	0.13 ±0.02	p=0.999
dark	0.11 ±0.02	0.12 ±0.03	p=0.993

762

Table 4. *ATP measurements taken at 20 h (coinciding with the exponential phase) for P. angustum S14 (wt) grown in Fe-replete and Fe-limiting conditions and p-values of a 1-way ANOVA comparing differences between light and dark conditions after a ln transformation in order to meet the assumptions of homogeneity of variance.* ***(n=4)***

***ATP** (fmol per 1000 cells)*	***Dark***	***Light***	***p-value***
Fe-replete	11.8 ± 1.47	8.2 ± 2.99	p = 0.1357
Fe-limiting	0.9 ± 0.04	0.9 ± 0.05	p = 1.0000

763

764

765 **10. Figures**

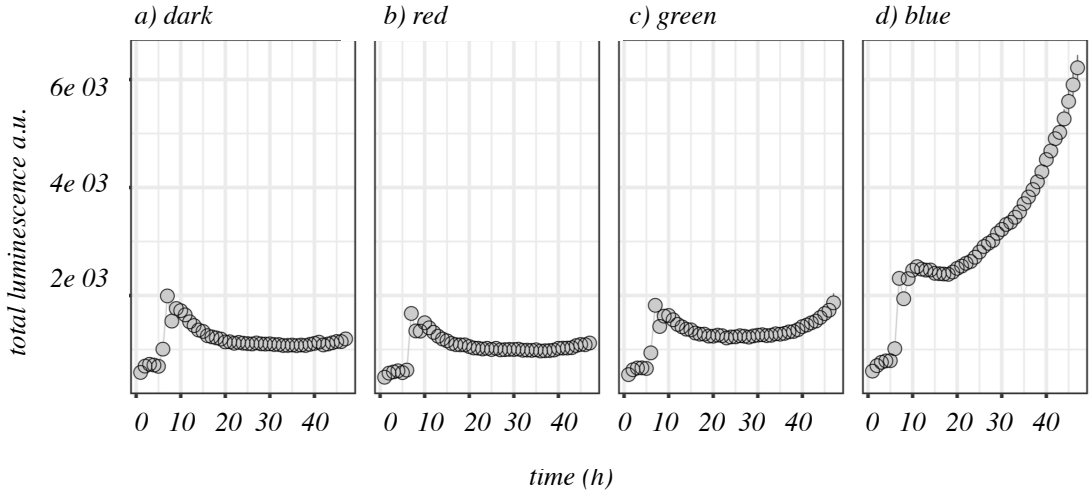

766

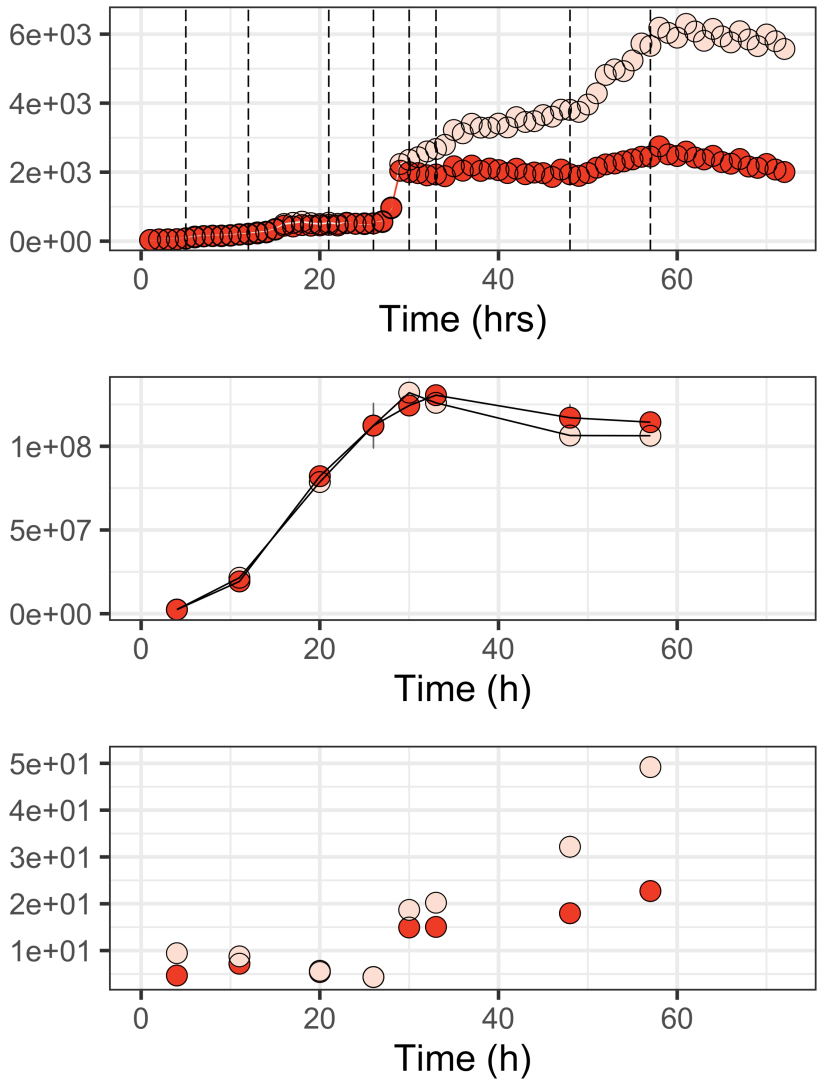
6e+03
4e+03
2e+03
0e+00
0
20
40
60
Time (hrs)
1e+08
5e+07
0e+00
0
20
40
60
Time (h)
5e+01
4e+01
3e+01
2e+01
1e+01
0
20
40
60
Time (h)

767

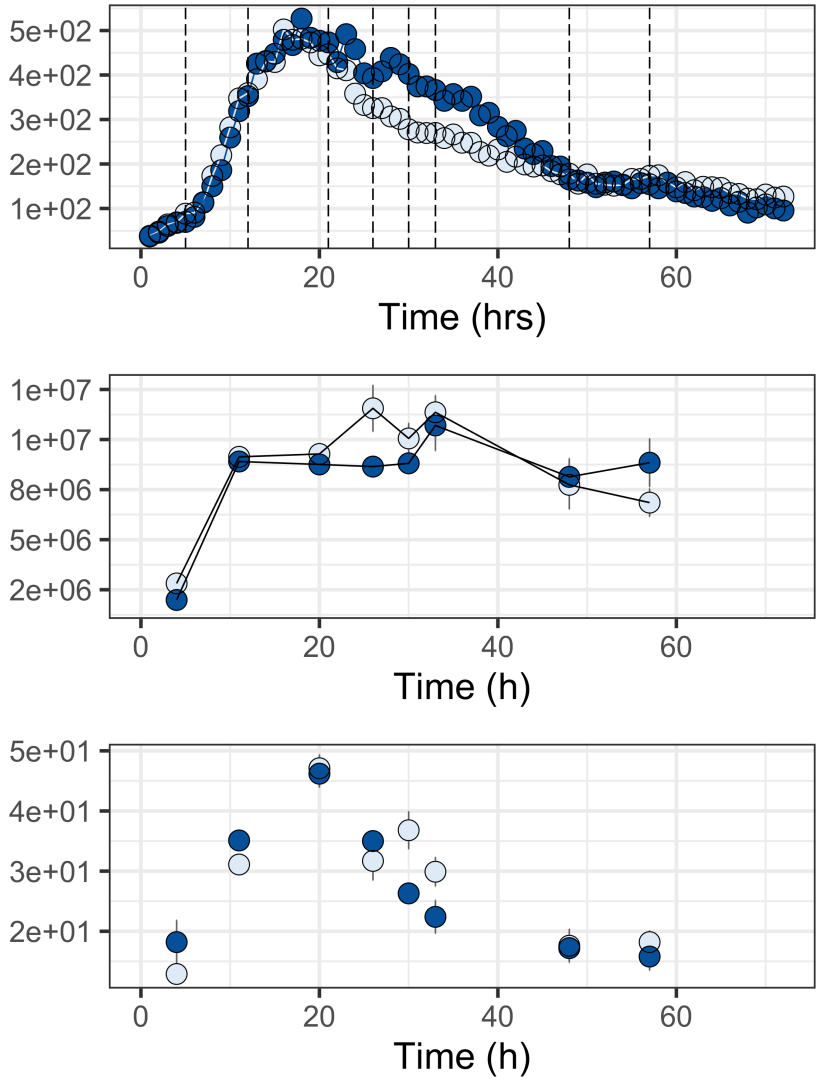
5e+02
4e+02
3e+02
2e+02
1e+02
0
20
40
60
Time (hrs)
1e+07
1e+07
8e+06
5e+06
2e+06
0
20
40
60
Time (h)
5e+01
4e+01
3e+01
2e+01
0
20
40
60
Time (h)

768

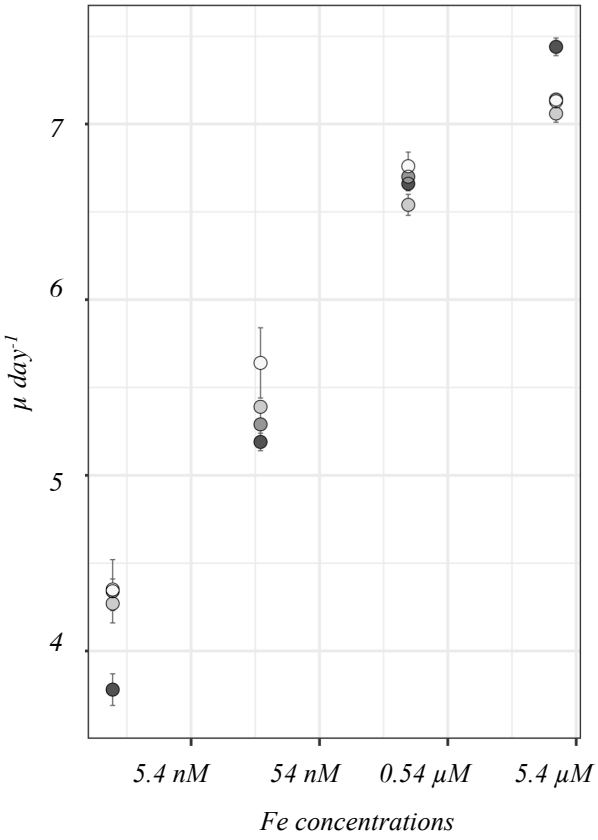
7
6
5
4
μ day-1
5.4 nM
54 nM
0.54 μM
5.4 μM
Fe concentrations

769

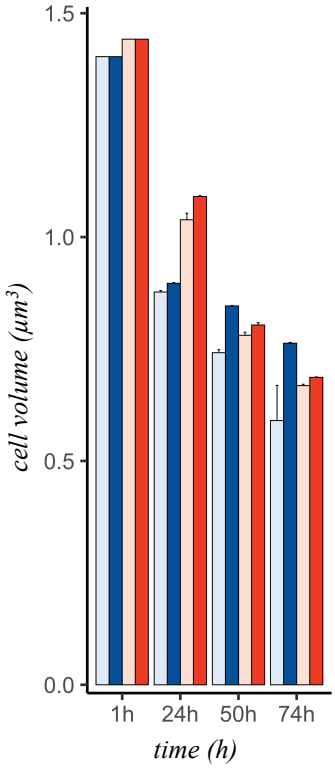
1.5
1.0
0.5
0.0
cell volume (μm3)
1h
24h
50h
74h
time (h)

770

11. Supplementary Information

11.1. Supplementary Text

Deriving growth rates and respiration rates from O_2 measurements

When bacterial cells are in exponential growth, both the bacterial respiration rate and growth rate are assumed to be constants. Therefore, if the initial bacterial cell abundance (N_0) is known, both the growth (μ) and respiration rates per cell (R_{cell}) can be derived from continuous dissolved oxygen concentration (O_2) measurements (Figure 15). While the relevance in the growth rate has been explained in the previous paragraphs, the respiration rate is an additional important parameter which provides an indication of the effect of Fe-limitation as 99% of Fe is expected to reside within the electron transport chain of heterotrophic bacteria and during respiration, a large portion of O_2 is consumed through the electron transport chain* where O_2 acts as the final electron acceptor.

O_2 measurements were taken from batch cultures using a SensorDish reader (Presens) equipped with 24 glass vials of 4.8 mL containing non-invasive O2 sensors (OxoDish). All growth and respiration experiments were conducted in triplicate (where one replicate represents one O_2 sensor vial). The entire setup was placed in an incubator at a constant temperature of 20°C. O_2 concentrations were derived from 10-min averages of quenched fluorescence measurements taken every 30 s over a period of 24 h. Each vial was calibrated using a two-point protocol. A 0 µM O_2 solution was prepared with a 1% Na_2SO_3 in Milli-Q water. A 100% oxygenated solution was prepared by bubbling air at a constant temperature for 2 h in Milli-Q water and left overnight with the lid open to allow exchange with air. O_2 concentrations in Aquil medium were further corrected for by taking into account the salinity of the medium (S = 35) using the solubility equation of Garcia and Gordon (1992). Blanks consisting of filtered Aquil medium (0.2 µm) were used to monitor for any significant drift from the O_2 sensors for the entire duration of the experiments (±24 h). A time window was carefully chosen in order to capture the exponential phase. In order to meet the assumption of a constant growth and respiration rate, care was taken to avoid the inclusion of any metabolic switches (Wolfe, 2005) that would result in a change in the oxygen consumption rate.

* other oxygen consuming entities are also known to occur such as NADH-oxidases but can be considered to be almost negligible in comparison to the electron transport chain.

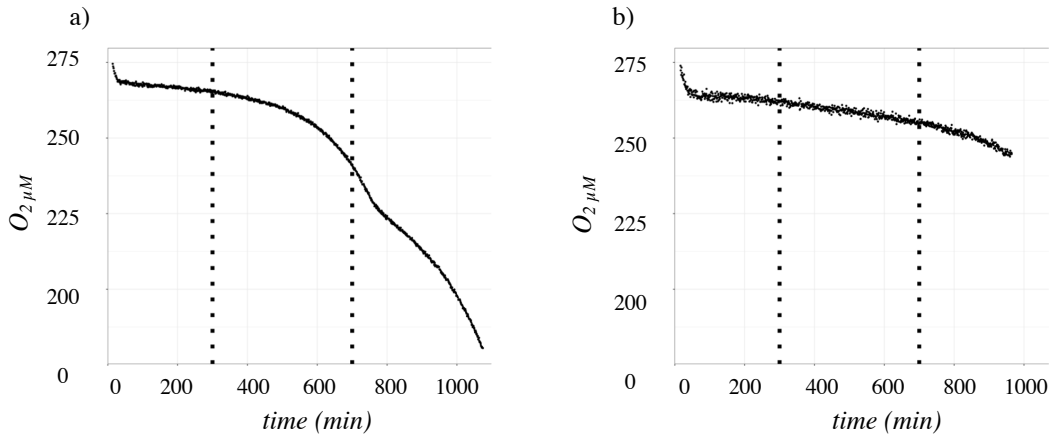

Supplementary Text Figure i. *O_2 consumption curves for P. angustum S14 grown in either Fe-replete (a) and Fe-limiting (b) conditions. Notice that two respiration curves can be observed for P. angustum S14 grown in Fe-replete conditions. Horizontal lines depict the window that was chosen to calculate the growth and respiration rate.*

An average of every 10 min was taken to derive the growth and respiration rates from the selected O_2 measurements. Changes in ΔO_2 concentrations over time were derived from the integral of the rate of change in O_2 over time using the following equation below:

$$\frac{dO_2}{dt} = -N_0\, R_{cell} \exp(\mu\, t)$$

The integration of the above equation gives:

$$\Delta O_2 = [O_2]_{ti} - [O_2]_{tf} = A\,(1 - \exp(\mu\, t))$$

with

$$A = \frac{-N_0\, R_{cell}}{\mu}$$

where $[O_2]_{ti}$ and $[O_2]_{tf}$ are the respective O_2 concentrations at the starting time point (ti) and at the final time point (tf). $\Delta O_2 = f(t)$ was fitted to the equation using sigmaplot software to derive μ and $A = \frac{-N_0\, R_{cell}}{\mu}$. A was then used to calculate R_{cell}.

Under Fe-limiting conditions, ΔO_2 was small and therefore the equation leads to an approximately linear relationship:

$$\Delta O_2 = N_0 R_{cell} t$$

where R_{cell} is derived from the slope of $\Delta O_2 = f(t)$ measurements which in this case can be defined from the following equation:

$$\mu = \frac{ln (N_f - N_0)}{(N_0 t_f)}$$

Where N_f is the final cell abundance at t_f derived from flow cytometry measurements. The agreement between experimental data and model fitting was then plotted in order to verify that the main assumptions of the model concerning a constant growth and respiration rate were met (Figure 16).

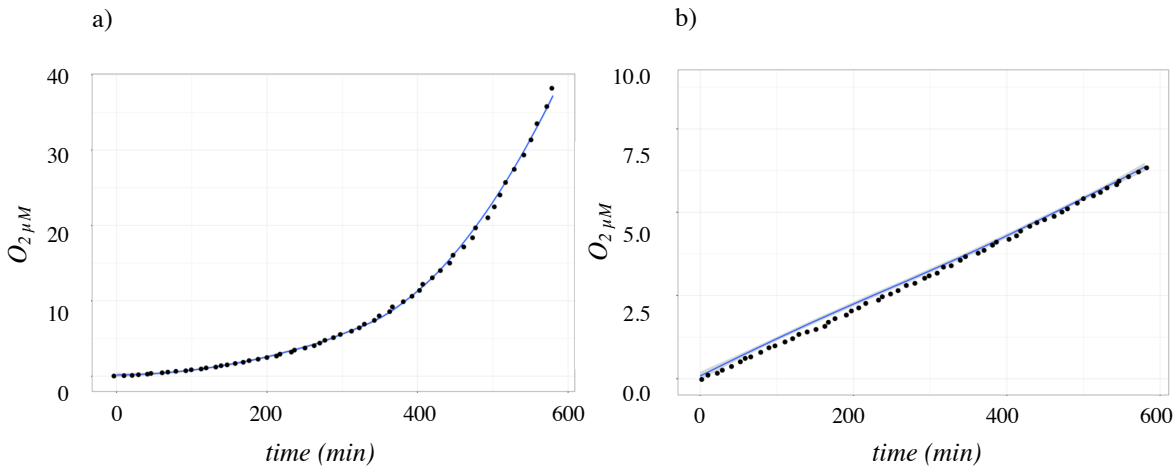

Supplementary Text Figure ii. *ΔO_2 consumption curves derived from the selected time window for P. angustum S14 grown in Fe-replete (left) and Fe-limiting (right) conditions. Fitting of the model (blue) with the experimental values shows the model's prediction for both the growth and respiration rates. The curves meet the assumption of a constant growth and respiration rate.*

11.2. Supplementary Tables

Supplementary Table 1. *A non-exhaustive list of culture-based studies testing the function of proteorhodopsin in heterotrophic bacteria and a brief summary of their findings.* (G-green tuned, B-blue tuned, N-no, Y-Yes, n/a-not available).

Bacterial Isolate	Phylum	PR type	Enhanced Growth?	Additional Findings	References
HTCC2207 (SAR92)	γ-proteobacteria	G	N	- No differences in growth or cell yield	Stingl et al., 2007
Vibrio campbellii AND4	γ-proteobacteria	G	Y	- Longterm survival in sterile seawater - PR expression is determined by nutrient limitation (dilutions) - Sigma factor RpoS plays key regulatory role	Gómez-Consarnau et al., 2010 Akram et al., 2013
Vibrio campbellii BAA-1116	γ-proteobacteria	G	Y	- Longterm survival under respiratory stress (sodium azide) - Enhanced ATP production - Sigma factor RpoS1 plays key regulatory role	Wang et al., 2012
Pelagibacter ubique HTCC1062 (SAR11)	α -proteobacteria	G	N	- Constitutively expressed - No differences in growth or cell yield	Giovannoni et al., 2005 Steindler, 2005
Dokdonia sp. MED134	Bacteriodetes	G	Y	- Upregulated in light - Enhanced growth rate and cell yield under low (0.6 mM[C]) and intermediate (1.1 mM[C] carbon concentrations - Enhanced Vitamin B1 acquisition - Upregulation of the glyoxylate shunt in light - Upregulation in transporters (alanine and phosphate) - Upregulation of Complex I of the electron transport chain	Gómez-Consarnau et al., 2007 Gómez-Consarnau et al., 2016 Palovaara et al., 2014 Kimura et al., 2011
Nonlabens marinus S1-08	Bacteroidetes	n/a	Y	- Enhanced growth rate and cell yield under 0.14 mM[C] - 3 rhodopsin types (H+, Na+ and Cl- pumps)	Yoshisawa et al., 2014
Polaribacter sp. MED152	Bacteroidetes	n/a	N	- Enhanced bicarbonate fixation and uptake	González et al., 2012
Psychroflexus torquis	Bacteroidetes	G	Y	- Enhanced growth and cell yield under hyposalinity stress	
ATCC 700755				- Constant expression post transcriptional upregulation by light and salinity - Increased yield in natural Antarctic sea ice in the presence of blue vs green light.	Feng et al., 2013 Feng et al., 2015 Burr et al., 2017
Hymenobacter nivis P3T	Bacteroidetes	n/a	Y	- Enhanced growth and cell yield	Terashima et al., 2018
P. angustum S14	γ-proteobacteria	B	N	- No difference in growth and cell yield - Decrease in Pirt's maintenance coefficient in light under high carbon concentrations - Increase in carbon yield	Courties et al., 2016

823

Supplementary Table 2. *Cell counts and ROS measurements taken at ±96 hours from ptr-luc (2n) grown in Fe-replete conditions in Aquil medium and acetate (6 mM[C]) and subjected to either dark conditions or constant blue light (n=2).*

Conditions	***Bacteria (cells mL^{-1})***	***ROS (r. f. u)***	***ROS 1000 cells^{-1}***
Acetate dark	*8.29 x10^{6}*	*7716*	*0.93*
	7.94 x10^{6}	*8276*	*1.04*
Acetate light	*3.13 x10^{6}*	*15388*	*4.92*
	3.53 x10^{6}	*13919*	*3.94*

824

Supplementary Table 3. *Growth rate (day^{-1}) and maximum cell abundance (abund.) of P. angustum S14 grown in a range of Fe-concentrations and subjected to either constant darkness (0%-blue) or 25, 50, 100% blue light in a white 96-well plate. (n=3).*

Growth rate (day^{-1})	**0% Blue**	**25% Blue**	**50% Blue**	**100% Blue**
5.4 µM	7.4 ± 0.1	7.1 ± 0.1	7.1 ± 0.1	7.1 ± 0.1
0.54 µM	6.7 ± 0.1	6.7 ± 0.1	6.5 ± 0.1	6.8 ± 0.1
54 nM	5.2 ± 0.1	5.3 ± 0.1	5.4 ± 0.1	5.6 ± 0.2
5.4 nM	3.8 ± 0.1	4.3 ± 0.2	4.3 ± 0.1	4.3 ± 0.1
Abund. (10^8 cells mL^{-1})	**0% Blue**	**25% Blue**	**50% Blue**	**100% Blue**
5.4 µM	1.4 ± 0.1	1.2 ± 0.1	1.3 ± 0.1	1.1 ± 0.2
0.54 µM	1.3 ± 0.1	1.2 ± 0.1	1.2 ± 0.1	1.2 ± 0.1
54 nM	0.7 ± 0.1	0.7 ± 0.1	0.8 ± 0.1	0.6 ± 0.1
5.4 nM	0.2 ± 0.1	0.3 ± 0.1	0.2 ± 0.1	0.2 ± 0.1

825

Supplementary Table 4. *Growth rate (day^{-1}) and maximum cell abundance (abund.) of Δpr grown in a range of Fe-concentrations and subjected to either constant darkness (0%-blue) or 25, 50, 100% blue light in a black 96-well plate. (n=3).*

Growth rate (day^{-1})	**0% Blue**	**25% Blue**	**50% Blue**	**100% Blue**
5.4 µM	6.8 ± 0.2	7.0 ± 0.2	6.9 ± 0.1	7.0 ± 0.2
0.54 µM	5.8 ± 0.1	6.2 ± 0.2	5.7 ± 0.3	5.4 ± 0.4
54 nM	4.6 ± 0.1	4.6 ± 0.2	4.9 ± 0.2	5.5 ± 0.1
5.4 nM	3.3 ± 0.1	3.3 ± 0.1	3.3 ± 0.1	3.2 ± 0.1
abund. (10^8 cells mL^{-1})	**0% Blue**	**25% Blue**	**50% Blue**	**100% Blue**
5.4 µM	1.2 ± 0.1	1.3 ± 0.1	1.1 ± 0.1	1.5 ± 0.2
0.54 µM	1.2 ± 0.1	1.2 ± 0.1	1.1 ± 0.1	1.3 ± 0.1
54 nM	0.3 ± 0.1	0.4 ± 0.1	0.3 ± 0.1	0.5 ± 0.1
5.4 nM	0.1 ± 0.1	0.2 ± 0.1	0.2 ±0.1	0.3 ± 0.1

826

Supplementary Table 5. *Mean cell volume (μm^3) of P. angustum S14 at several time points grown in 6mM[C] of glucose in either Fe-replete or Fe-limiting conditions and subjected to constant darkness or blue light. At 1 hour, cell size was measured from acclimated cells grown overnight in glucose and Fe-replete conditions. 24 hours coincides with the end of the exponential growth phase and start of the exponential phase. 50 hours coincides with peak proteorhodopsin expression and 75 hours when the expression of proteorhodopsin is in decline. Significant differences between light and dark conditions for each time point are shown in bold. (n=3).*

Conditions	1h	24h	50h	74h
Fe-rep + dark	1.44	1.09 ± 0.00	0.80 ±0.01	0.69 ± 0.00
Fe-rep + light	1.44	1.04 ±0.02	0.78 ±0.01	0.67 ± 0.00
		p= 0.0056	p= 0.0707	p= 0.9860
Fe-lim + dark	1.35	0.90 ± 0.00	0.85 ± 0.00	0.76 ± 0.00
Fe-lim + light	1.35	0.88 ± 0.00	0.74 ± 0.01	0.59 ± 0.08
		p= 0.3343	**p<0.0001**	p= 0.0573

11.3. Supplementary Figures

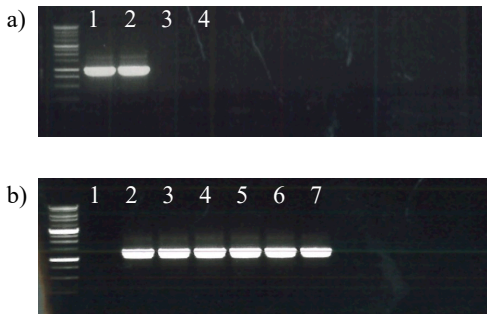

Supplementary Figure 1. PCR results confirming the formation of the mutants Δpr (a) and ptrluc (b). **a)** PCR products of the presence or absence of the proteorhodopsin gene (800bp) where columns 1-2 represents the wt with the presence of the proteorhodopsin gene and columns 3-4 represents the Δpr with the absence of that gene. **b)** PCR products of the proteorhodopsin-luciferin construct ptrluc (1169 bp) where the first column represents the wt (with the absence of luciferin) and columns 2-7 represents ptrluc containing the construct.

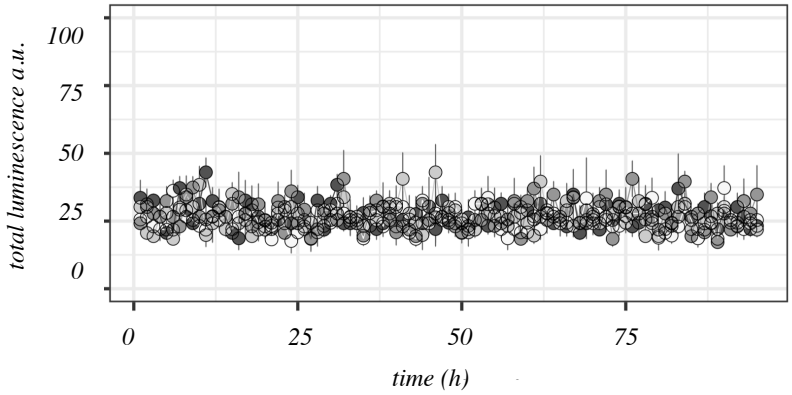

Supplementary Figure 2. Blanks containing Aquil medium, luciferin (μM) and a range of light concentrations (0, 10, 50, 100 %) placed in a black 96-well plate for a period of 96-hours. The use of a black plate removed the differences found in the presence or absence of light when using a white plate.

831

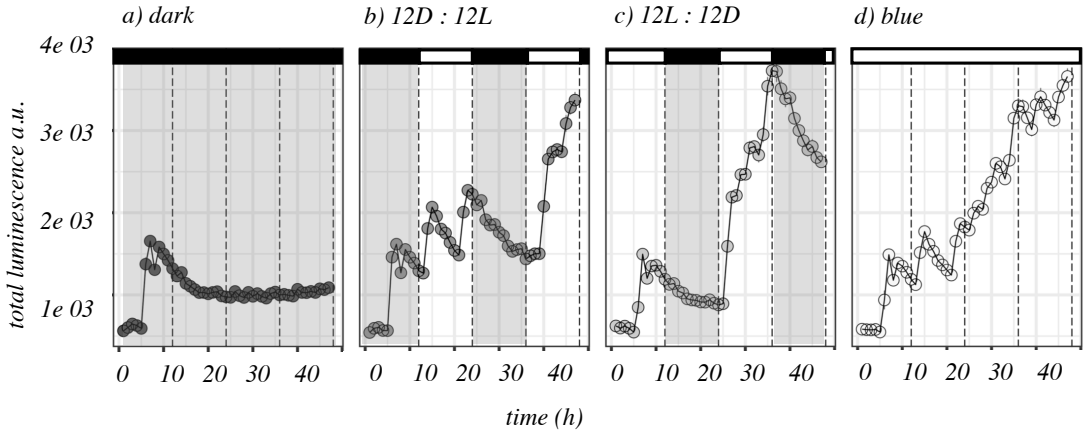

832

Supplementary Figure 3. PTR-luc in Aquil medium and 6mM[C] glucose, subjected to either (a) no light, (b) 12 h dark – 12 h light cycles, (c) 12 h light – 12 h dark cycles (12L:12D) and (d) constant blue light (50%). After 8 hours, an increase in luminescence is observed regardless of the presence or absence of light. After 24 hours, respective increase or decrease in luminescence is observed when light is either present or absent. ***(n=5)***

833

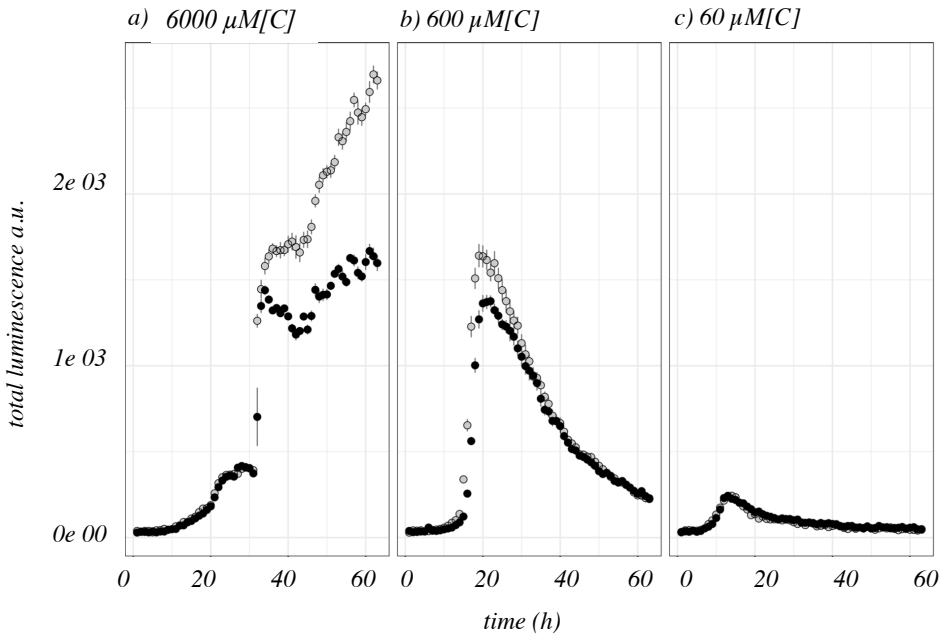

Supplementary Figure 4. PTR-luc grown in Fe-replete conditions in Aquil medium and (a) (6000 μM[C] (b) 600 µM[C], and (c) 60 µM[C] glucose and subjected to either dark conditions (grey circles) or constant blue light (white circles). ***(n=5)***

834

a) Acetate

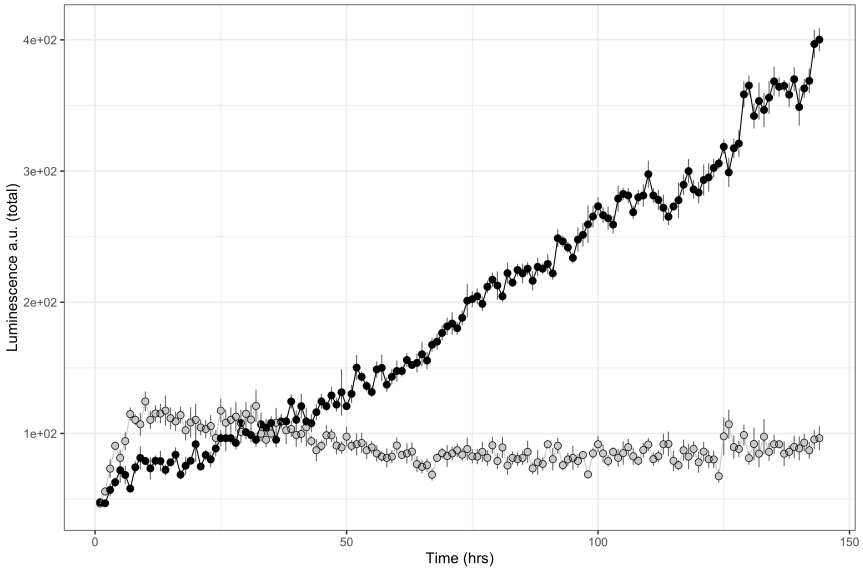

b) Serine

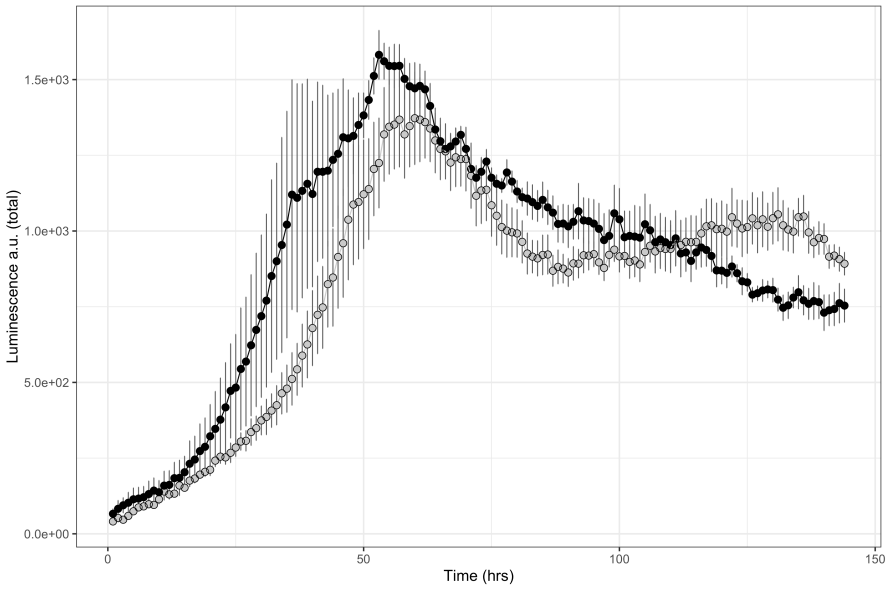

Supplementary Figure 5. PTR-luc grown in Fe-replete conditions in Aquil medium containing (a) 6mM[C] acetate (b) 6mM[C] serine and subjected to either dark (black) or constant blue light (grey). The high standard deviation present in serine is likely a result of a high production of EPS which formed particles that interfered with the luminescence measurements.

835

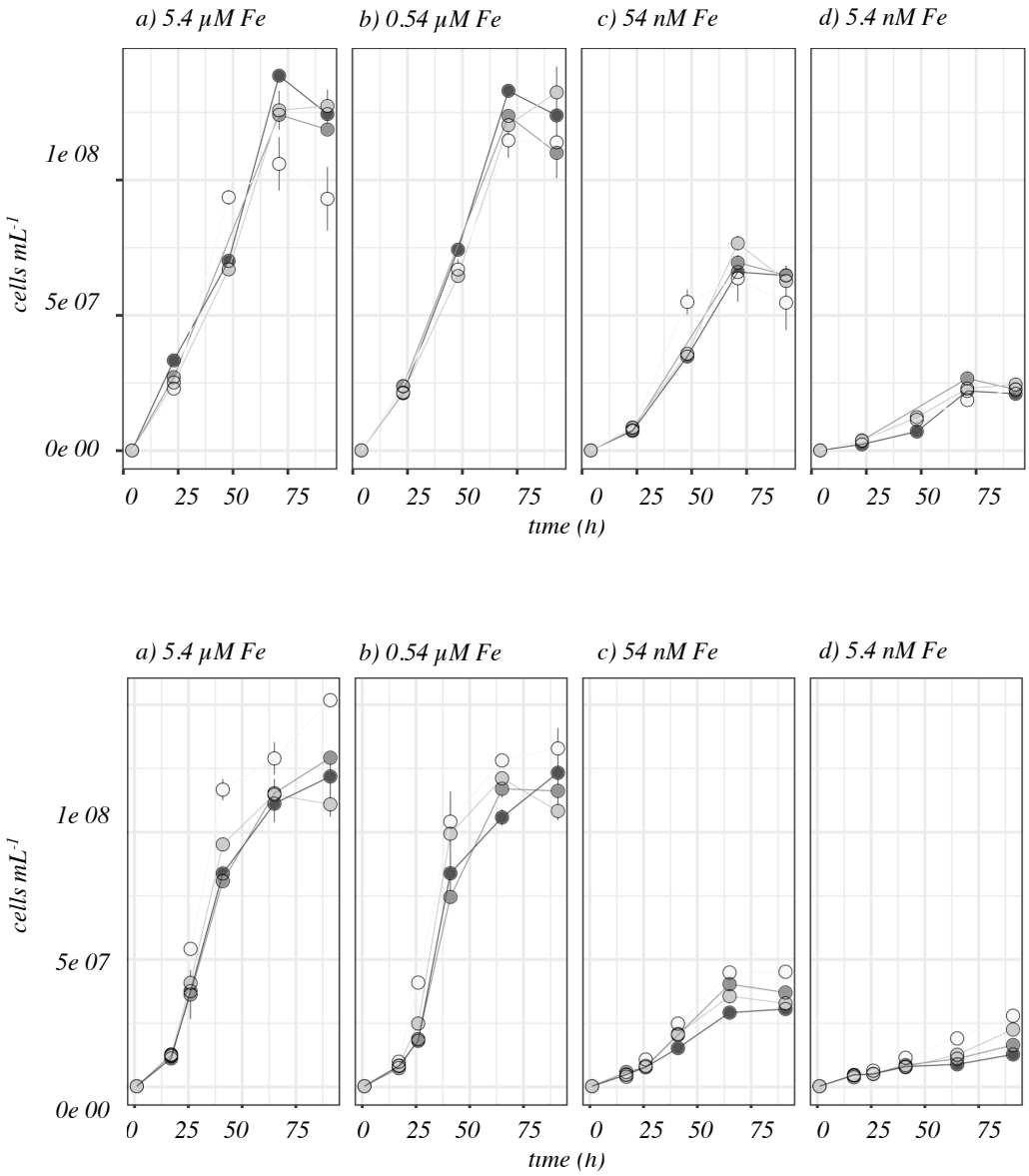

Supplementary Figure 6. *Growth curves of P. angustum S14 wt (top) and Δpr (bottom) grown in Aquil with 6mM[C] glucose, subjected to (a) 5.4 µM, (b) 0.54 µM, (c) 54 nM, (d) 5.4 nM of Fe and 0, 25, 50, 100% blue light (dark grey, grey, light grey and white circles).* ***(n=3)***

836